Penerbit Akademia Baru

Malaysian Journal on Composites Science and Manufacturing

Journal homepage:
https://www.akademiabaru.com/submit/index.php/mjcsm/
ISSN: 2716-6945

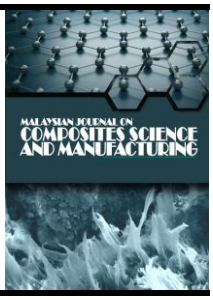

Parametric Study and Characterization of Nitrogen-Doped Carbon Quantum Dots Synthesized via Hydrothermal Method

Open Access

Nurul Ayunni Abdul Latif[1,2], Jeefferie Abd Razak[1,*], Wan Putri Najihah Zulkarnain[1], Rose Farahiyan Munawar[1], Noraiham Mohamad[1], Intan Sharhida Othman[1], Poppy Puspitasari[3]

[1] Fakulti Teknologi dan Kejuruteraan Industri dan Pembuatan, Universiti Teknikal Malaysia Melaka, Hang Tuah Jaya, Durian Tunggal, Melaka 76100, Malaysia
[2] Politeknik Merlimau Melaka, KM2.5, Jalan Merlimau-Jasin, 77300, Merlimau, Melaka, Malaysia.
[3] Mechanical and Industrial Engineering Department, Engineering Faculty, Universitas Negeri Malang, Jl. Semarang, No. 5, Malang, East Java, Indonesia

ARTICLE INFO

Article history:
Received 15 February 2025
Received in revised form 26 March 2025
Accepted 26 March 2025
Available online 30 March 2025

Keywords:

N-CQDs, hydrothermal synthesis, photoluminescence, green chemistry, Tauc plots, functional filler

ABSTRACT

Carbon quantum dots (CQDs) are zero-dimensional nanomaterials known for their chemical stability, water dispersibility, low cytotoxicity, small size, biocompatibility, and photoluminescence. This study reports the synthesis of nitrogen-doped carbon quantum dots (N-CQDs) using urea and citric acid derived from calamansi lime via a simplified hydrothermal method. A 2^3 full factorial Design of Experiments (DOE) was employed to optimize synthesis parameters, comprising temperature, reaction time, and precursor ratio, with optimal conditions identified as 140 °C, 2 hours, and a 1:1 precursor ratio. The resulting N-CQDs exhibited strong photoluminescence, excellent colloidal stability, and particle sizes ranging from 5 to 10 nm. Tauc plot analysis indicated bandgap energies up to 5.81 eV, influenced by particle size and quantum confinement. UV-Vis and FTIR spectroscopy confirmed the absorption behavior and the presence of nitrogen and oxygen functional groups, respectively, while photoluminescence measurements showed intense emission. FESEM, TEM, and EDX analyses revealed uniform spherical morphology and confirmed successful nitrogen doping. Overall, the tunable surface chemistry and optical properties of N-CQDs make them promising for bioimaging, sensing, and optoelectronics applications. At the same time, the sustainable, cost-effective hydrothermal synthesis method supports scalable production for use as functional fillers in nanocomposites.

1. Introduction

Carbon quantum dots (CQDs) are a class of zero-dimensional nanomaterials that have attracted significant attention due to their exceptional optical, electronic, and structural properties. These

* *Corresponding author.*
E-mail address: jeefferie@utem.edu.my (Jeefferie Abd Razak)
E-mail of co-authors: ayunnilatif@gmail.com, jihahzul18@gmail.com, rosefarahiyan@utem.edu.my, noraiham@utem.edu.my, intan_sharhida@utem.edu.my, poppy@um.ac.id

https://doi.org/10.37934/mjcsm.16.1.111124

properties include tunable photoluminescence, high water solubility, excellent biocompatibility, and low cytotoxicity, making CQDs highly suitable for a wide range of applications, such as bioimaging, chemical sensing, drug delivery, and optoelectronic devices [1]. With sizes typically less than 10 nanometres, CQDs exhibit quantum confinement effects, which influence their optical characteristics, further enhancing their potential in bioimaging, sensing, optoelectronics, and functional filler for nanocomposites [2].

Traditional methods of synthesizing CQDs often involve energy-intensive processes and the use of hazardous chemical reagents, limiting their sustainability and large-scale applicability [3]. To address these limitations, hydrothermal synthesis has emerged as a more environmentally friendly alternative, utilizing renewable carbon precursors such as citric acid, glucose, and various biomass sources [4]. Among various doping strategies, nitrogen doping is particularly effective in enhancing the optical and electronic properties of CQDs. By introducing additional energy states within the band structure, it significantly improves fluorescence quantum yields and stability [5]. As highlighted by Vercelli *et al.* [6], nitrogen doping can enhance the quantum yield of CQDs, boosting their fluorescence properties. Similarly, Šafranko *et al.* [7] demonstrated that doping modifies the band gap of CQDs, either broadening or narrowing it, thus influencing their electrical conductivity and charge carrier dynamics.

Therefore, this study explores on the hydrothermal synthesis of nitrogen-doped carbon quantum dots (N-CQDs) using citric acid derived from calamansi lime as the carbon precursor and urea as the nitrogen source. Calamansi lime, a locally available and renewable resource, offers an efficient and sustainable alternative for CQD synthesis in line with green chemistry principles. The nitrogen incorporation is expected to enhance the photoluminescence intensity, stability, and surface chemistry of the N-CQDs, enhancing their suitability for optoelectronic, biomedical, and functional filler for nanocomposites applications [8].

To optimize the synthesis process, this study employs a statistical Design of Experiment (DOE) approach, specifically the 2^3 full factorial method, to assess the effects of key synthesis parameters, including reaction temperature, precursor ratio, and synthesis duration [9]. The resulting N-CQDs are characterized using several analytical techniques, such as UV-VIS absorption spectroscopy to determine optical band gaps, photoluminescence (PL) spectroscopy to analyze fluorescence behaviour, Fourier-transform infrared (FTIR) spectroscopy to identify surface functional groups, and field emission scanning electron microscopy (FESEM) and transmission electron microscopy (TEM) for morphological analysis.

By optimizing the synthesis conditions and characterizing the resulting N-CQDs, this study aims to establish a direct correlation between synthesis parameters, particle size, and photoluminescence properties. The findings will contribute to the expanding body of research on sustainable nanomaterial synthesis and offer valuable insights into the potential applications of N-CQDs in bioimaging, chemical sensing, and next-generation optoelectronic devices as functional fillers in nanocomposites applications.

2. Methodology

2.1 Material

Urea (Sigma-Aldrich, CAS number 57-13-6) was used as the nitrogen precursor, and citric acid, derived from calamansi lime purchased from the local market, served as the carbon precursor for synthesizing nitrogen-doped carbon quantum dots (N-CQDs). Figure 1 illustrates the schematic representation of the synthesis process, highlighting urea as the nitrogen source and citric acid from calamansi lime as the carbon source.

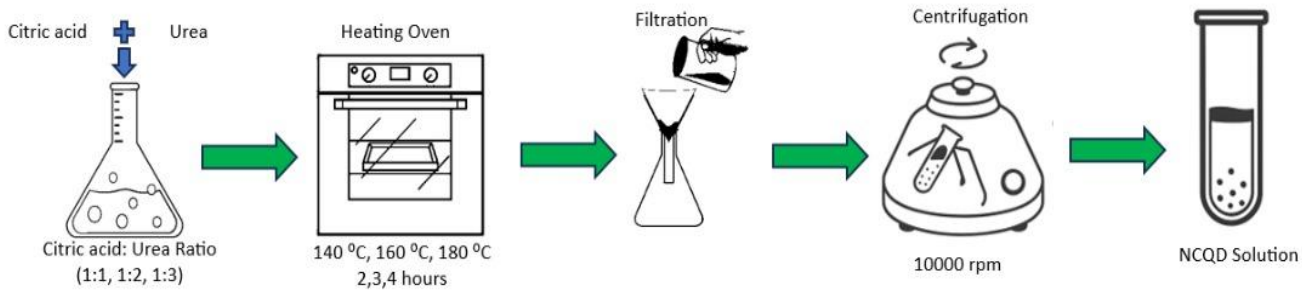

Fig. 1. Schematic illustration for the synthesis of CQDs from urea and citric acid (Calamansi Lime)

2.2 Synthesis of N-CQDs

The N-CQDs were synthesized using a hydrothermal method. A parametric study of the reaction conditions was conducted using a two-level full factorial Design of Experiment (DOE) approach, facilitated by the Design Expert Software (Stat-Ease, version 13.0.5). The study varied factors such as temperature (140°C, 160°C, 180°C) as X_1, reaction time (2, 3, 4 hours) as X_2, and the urea-to-citric acid ratio (1:1, 1:2, 1:3) as X_3. The synthesis was carried out in a sealed autoclave to enhance reaction efficiency, following a 2^3 full factorial DOE design with 3 repetitions at the centre point, across 11 experimental sets. The key parameters for N-CQD synthesis in the two-level full factorial study are summarized in Table 1, while the specific parametric combinations are listed in Table 2. The parametric study on the hydrothermal synthesis of N-CQDs used the band-gap results, determined through Tauc-Plot analysis of the UV-Vis spectroscopy, as the main response.

Table 1
Key parameters for N-CQDs synthesis

Parameter	Range	Parameter Code
Reaction Temperature	140 – 180 ◦C	X_1
Reaction Time	2 – 4 *hrs.*	X_2
Precursor Concentration Ratio (Urea: Citric Acid)	1:1, 1:2, 1:3	X_3

Table 2
Parametric combination for N-CQDS synthesis using a two-level full factorial method

Sample	X_1	X_2	X_3
1	140	2	1:1
2	180	2	1:1
3	140	4	1:1
4	180	4	1:1
5	140	2	1:3
6	180	2	1:3
7	140	4	1:3
8	180	4	1:3
9	160	3	1:2
10	160	3	1:2
11	160	3	1:2

2.3 Characterization Techniques

To investigate the properties of nitrogen-doped carbon quantum dots (N-CQDs), several characterization techniques were employed. UV-Vis absorption spectroscopy was used to examine the absorption spectrum of the N-CQDs, which allowed for the estimation of their band gap [10]. This technique provides important insights into the electronic transitions within the N-CQDs. The UV-Vis analysis was conducted using a Shimadzu UV-1900i Plus spectrophotometer. An aliquot of N-CQDs was first diluted (0.50 ml N-CQDs with 40 ml distilled water) and centrifuged at 10,000 *rpm* for 15 minutes to obtain a clear supernatant for UV-VIS testing, which was then transferred to a cuvette for analysis. The sample was scanned over 200–800 nm to record the absorption spectrum.

Photoluminescence (PL) spectroscopy was employed to measure fluorescence intensity and emission spectra, which are essential for understanding the optical properties of the N-CQDs, particularly their potential applications in bioimaging and sensing. The PL spectrum provides insights into the emission behaviour under varying excitation conditions [10]. An aliquot of N-CQDs was first diluted (0.50 ml N-CQDs with 40 ml distilled water) and centrifuged at 10,000 rpm for 15 minutes to obtain a clear supernatant for PL testing. PL analysis was conducted using a PerkinElmer LS55 fluorescence spectrometer, which recorded 300 nm to 800 nm spectra under optimized excitation conditions.

Fourier-transform infrared (FTIR) spectroscopy was used to identify the surface functional groups of the nitrogen-doped carbon quantum dots (N-CQDs) [11]. This technique provided valuable information on the chemical bonding and surface chemistry of the material, confirming the presence of nitrogen-containing functional groups, which indicate successful nitrogen doping. FTIR analysis was performed using the attenuated total reflectance (ATR) method on a BRUKER Alpha II FTIR spectrometer, with a scanning range of 4000 to 400 cm^{-1} to identify the characteristic absorption bands.

For morphological observation, the field emission scanning electron microscopy (FESEM) and transmission electron microscopy (TEM) were employed to analyze the morphological and structural characteristics of the N-CQDs. These imaging techniques revealed that the N-CQDs exhibited a uniform spherical shape, smaller dots size, and crystalline structure [12-13]. For FESEM with EDX analysis, about 5 ml of raw N-CQDs was mixed with 45 ml of acetone to facilitate the removal of excess organic material. The solution was then centrifuged at 10,000 rpm for 15 mins, and the collected sample was dried in an oven at 60˚C for 3 hours. FESEM observation was using Hitachi SU5000 at secondary and backscattered mode. TEM imaging was conducted using Talos L120C at a resolution of 0.20 nm at 120 kV, under the magnification range from 35x to 910x.

3. Results

3.1 Optimization of Synthesis Parameters

The optimal synthesis conditions for nitrogen-doped carbon quantum dots (N-CQDs) were determined using a Design of Experiments (DOE) approach, focusing on three critical parameters: reaction temperature, reaction time, and the urea-to-citric acid ratio. The DOE analysis identified the ideal combination as a reaction temperature of 140 °C, a reaction time of 2 hours, and a 1:1 ratio of urea to citric acid. Under these conditions, the synthesized N-CQDs demonstrated excellent photoluminescence and a uniform dots size distribution. These results were consistent with findings in previous studies, where the optimization of synthesis parameters significantly affected the structural and optical properties of carbon quantum dots [14]. The optimization process indicated that these conditions led to the highest desirability value for the synthesis of N-CQDs with a bandgap

of 5.813 eV, which is ideal for their potential applications in optoelectronics and bioimaging as a functional filler for nanocomposites. The DOE results indicated that these synthesis conditions were optimal for producing N-CQDs with enhanced fluorescence, which is attributed to smaller particle sizes that result in the quantum confinement effect.

During the DOE optimization, several trials were conducted with varying temperatures, precursor ratios, and reaction times. It was observed that higher temperatures (greater than 160°C) resulted in the formation of larger dot sizes, which led to a reduced band gap and lower photoluminescence. Similarly, lower temperatures (below 140°C) were not as effective, as they resulted in lower quantum yields and less efficient fluorescence. These findings are consistent with the quantum confinement effect, where smaller particle sizes lead to higher energy states, increasing the material's photoluminescence.

Furthermore, the urea to citric acid ratio played a crucial role in the synthesis. The ratio of 1:1 produced the most stable and uniform N-CQDs, with no significant aggregation or defects. When the ratio was altered to 1:2 or 1:3, the resulting N-CQDs exhibited poorer dispersion and lower fluorescence, likely due to excess urea disrupting the nitrogen doping process or causing other by-products that reduced the optical performance of the N-CQDs.

The following Figure 2 shows a three-dimensional response surface plot that illustrates the relationship between the synthesis parameters and the band gap of the N-CQDs. The plot highlights the optimal synthesis conditions (140°C, 2 hours, 1:1 urea to citric acid ratio) that maximize the band gap of 5.18 eV.

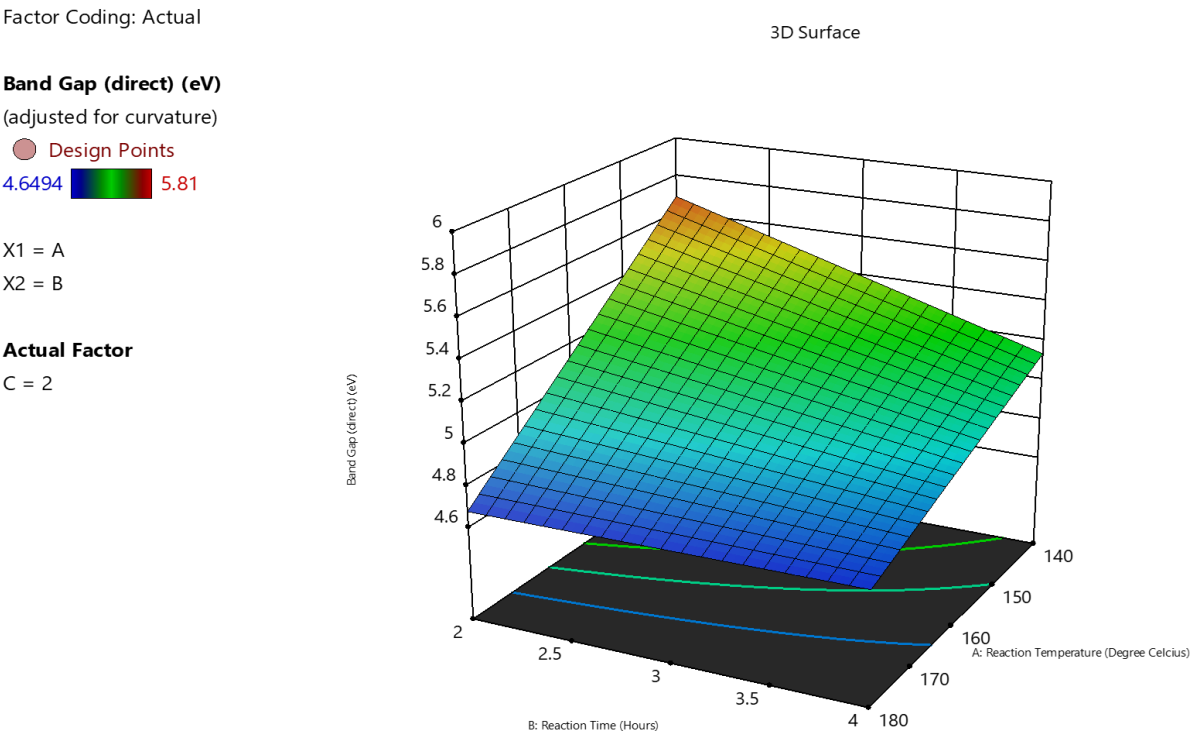

Fig. 2. Three-Dimensional Response Surface Plot of Bandgap Response in Calamansi Lime N-CQD Synthesis

Table 3 summarizes the optimization results from the response surface methodology (RSM), detailing the experimental conditions that led to the highest band gap.

Table 3
Optimization Result of RSM on Synthesis of Calamansi Lime N-CQD

Parameter	Units	Goal	Level		Optimization Result
			Lower	Upper	
Reaction Temperature	°C	is in range	140	180	140
Reaction Time	Hours	is in range	2	4	2
Precursor Concentration	Ratio (Urea: Citric Acid)	is in range	1:1	3:1	1:1
Bandgap (direct)	eV	maximize	4.6494	5.81	5.813

Figure 3 presents the ramp graphical view, showing the trend of photoluminescence properties such as band gap concerning the changes in synthesis parameters (temperature, reaction time, and precursor ratio). It helps visualize the variation in optical properties and supports the selection of the optimal conditions.

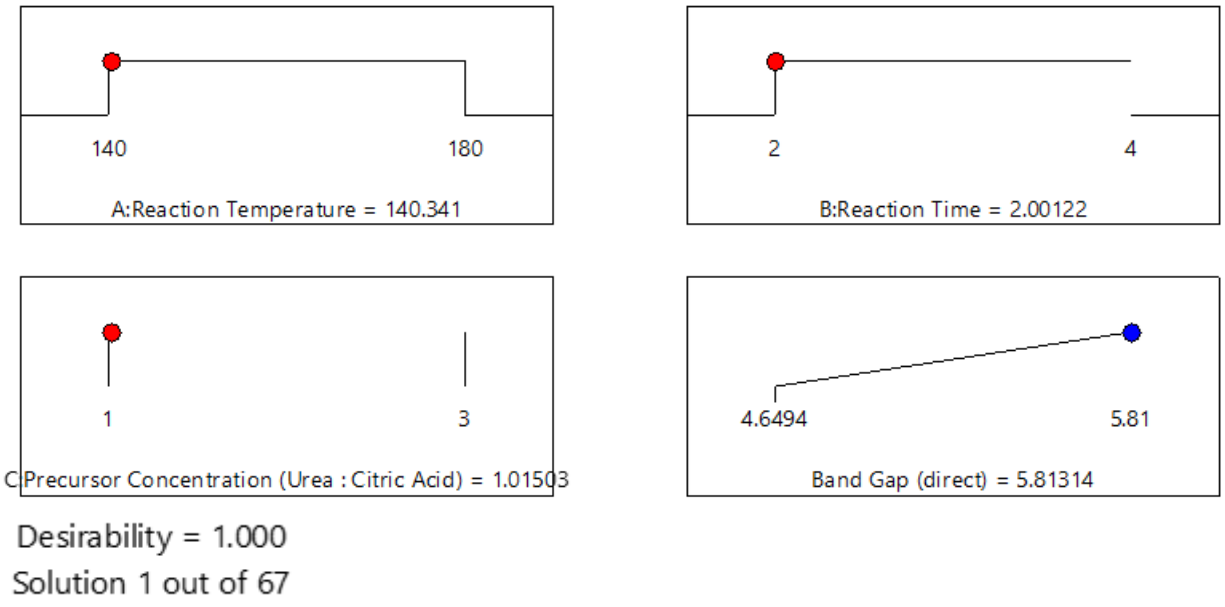

Fig. 3. Optimization Results of Calamansi Lime N-CQD Synthesis in Ramp Graphical View

Figure 4 illustrates the histogram view, depicting the material's ability to absorb and emit light across different experimental setups. It clearly shows the peak in band gap when the 1:1 urea to citric acid ratio and 140°C temperature are used.

In conclusion, the DOE analysis provided critical insights into the synthesis of N-CQDs, and the results indicate that 140°C, 2 hours, and a 1:1 urea to citric acid ratio are the optimal conditions for obtaining N-CQDs with high photoluminescence and uniform dot size distribution. These findings were further validated through response surface analysis, and the quantum confinement effect was confirmed, demonstrating the correlation between particle size and band gap.

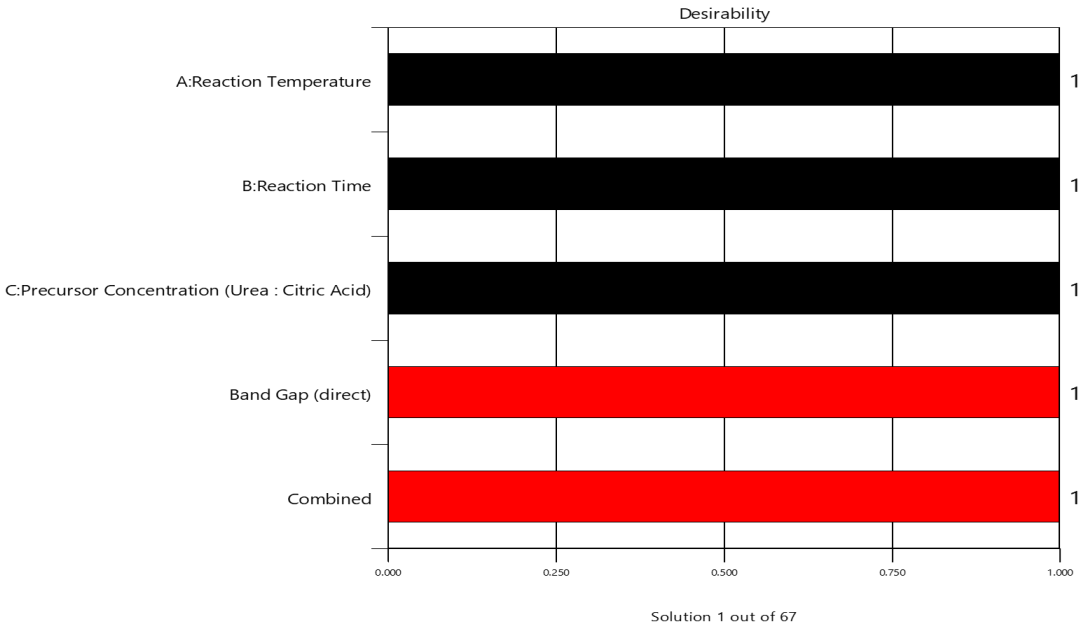

Fig. 4. Optimization Results of Calamansi Lime N-CQD Synthesis in Histogram View

3.2 Optical and Structural Properties

The UV-VIS absorption spectrum of the N-CQDs revealed characteristic absorption peaks, which were analyzed to determine the optical band gap of the material. The band gap was determined using the Tauc plot method, resulting in an optical maximum band gap of 5.813 eV. The Tauc plot analysis involved plotting $(\alpha h\nu)^{1/2}$ versus $h\nu$, where α is the absorption coefficient, and $h\nu$ is the photon energy (h = Planck's constant = 6.626 x 10^{-34} J.s; ν = frequency of the electromagnetic wave associated with photon). By extrapolating the linear portion of this plot, the band gap was identified. This method proved effective in determining the electronic structure and bandgap of the synthesized nanomaterials. In this study, the bandgap values ranged from a minimum of 4.6494 eV to a maximum of 5.813 eV, depending on the experimental conditions. These findings are consistent with previous research on carbon-based quantum dots, such as that by Sharma and Chowdhury (2023) [14], which highlights the influence of synthesis parameters on electronic properties. The maximum band gap was observed when the N-CQDs were synthesized under optimal conditions, resulting in a smaller dot size. Conversely, the minimum band gap was associated with larger N-CQDs. The relationship between the band gap and the size of the particles is governed by the quantum confinement effect, where smaller particles exhibit larger band gaps due to more pronounced electronic confinement. This effect significantly influences the photoluminescence (PL) and optical properties of the material [15].

Given the importance of photoluminescence characteristic for applications such as bioimaging and sensing, we selected the maximum band gap (5.813 eV) for further analysis. This choice was based on the correlation between a larger band gap and enhanced photoluminescence properties. Smaller particle sizes with larger band gaps tend to emit higher intensity fluorescence, as the confined electrons exhibit more efficient recombination. These properties are desirable for applications requiring high fluorescence intensity and stable emission in various optoelectronic devices [16].

3.2.1 Tauc Plot Calculation: Direct or Indirect Transition

For the direct band gap calculation, n was chosen to be 1/2 (Equation 1). This is appropriate for materials with direct band gap transitions, where the electron transition occurs without the involvement of phonons, as seen in some quantum dots and nanomaterials. For direct transition, the Tauc plot is given by:

$$(\alpha h\nu)^{1/2}=A(h\nu-E_g) \quad (1)$$

Where A is a constant and E_g is the direct band gap.

However, for N-CQDs, which exhibit size-dependent quantum confinement effects, the indirect band gap transition was also considered. In this case, the exponent n is 2 (Equation 2), suitable for materials with an indirect transition, where the electron must interact with a phonon to transition between the valence and conduction bands. For indirect transition, the Tauc plot is given by:

$$(\alpha h\nu)^{2}= A\ (h\nu-E_g) \quad (2)$$

Where A is a constant and E_g is the indirect band gap.

The decision to choose between the direct and indirect band gap calculation was made based on optical absorption characteristics observed in the UV-VIS absorption spectrum. The direct transition model was more appropriate for N-CQDs in this study due to their typical electronic structure, which behaves similarly to direct band gap semiconductors. Figure 5 displays the UV-VIS absorption spectrum of the N-CQDs and the corresponding Tauc plot. The plot clearly shows the linear region used to calculate the direct band gap, which was found to be 5.813 eV for the N-CQDs synthesized under the optimized conditions.

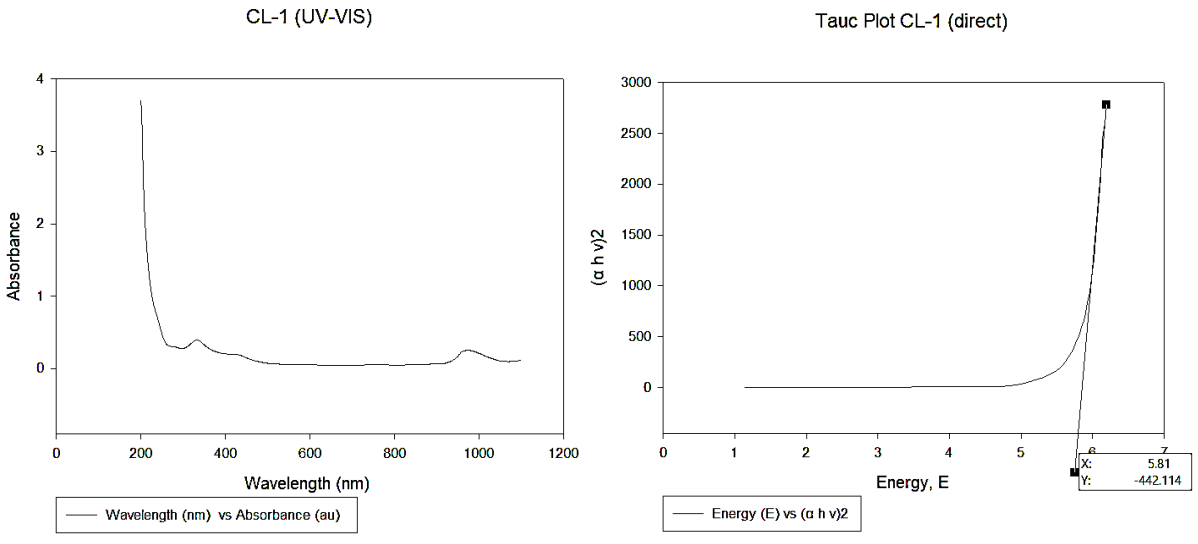

(a) (b)

Fig. 5. UV-VIS Absorption Spectrum and Tauc Plot of N-CQDs

The photoluminescence (PL) spectrum further confirmed the relationship between band gap and photoluminescence. The N-CQDs exhibited excitation-dependent fluorescence, with the maximum emission peak at 554 nm when excited at 500 nm. This behavior is typical of carbon quantum dots, where the emission spectrum shifts depending on the excitation wavelength, indicating a tunable photoluminescence property [16]. As particle size decreased, the emission intensity increased, which is consistent with the quantum confinement effect. Figure 6 illustrates the PL emission spectra at various excitation wavelengths, showing the typical excitation-dependent fluorescence behavior.

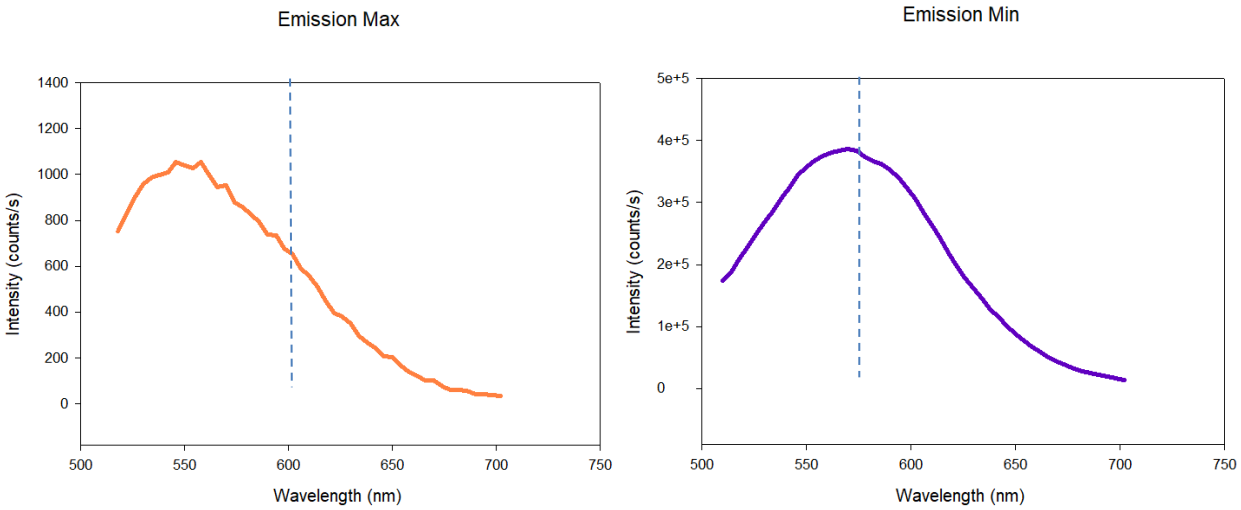

(a) (b)

Fig. 6. Photoluminescence Spectrum of N-CQDs

The FTIR spectroscopy as shown in Figure 7 revealed nitrogen-containing functional groups such as amines and carboxyl groups, confirming that nitrogen doping was successfully incorporated into the carbon matrix of the N-CQDs. Nitrogen doping enhances the optical and electronic properties of the quantum dots by introducing additional energy states within the band gap. This increases the material's stability and fluorescence efficiency, which are critical for applications such as sensing and bioimaging. The FTIR spectra highlight the presence of functional groups that verify the successful nitrogen doping and surface modification of the N-CQDs [17-18].

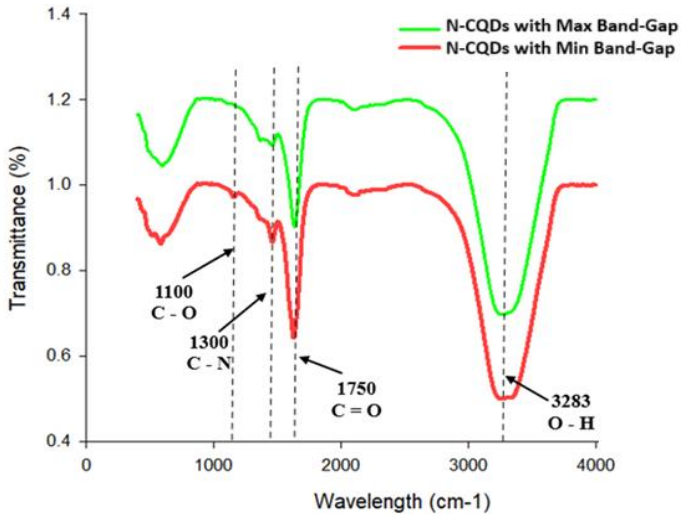

Fig. 7. FTIR Spectrum of N-CQDs

The morphology and particle size distribution of the N-CQDs were analyzed using FESEM and TEM. Both imaging techniques revealed that the N-CQDs were spherical with sizes ranging from 5 to 10 nm, which aligns with the desired size range for quantum dots used in optoelectronics [19, 20]. The particle size distribution was relatively uniform, and the crystalline structure of the N-CQDs was confirmed through TEM analysis. The smaller particle sizes corresponded to the larger band gap and enhanced photoluminescence observed [21-22]. Figures 8, 9, 10, and 11 include FESEM and TEM images showing the uniform spherical morphology and crystalline structure of the N-CQDs.

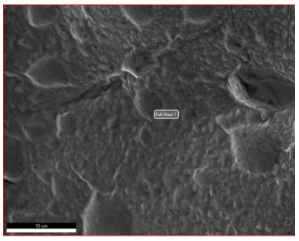

(a)

eZAF Quant Result - Analysis Uncertainty: 10.84 %

Element	Weight %	Atomic %
C	30.8	37.6
N	40.5	42.4
O	21.0	19.3
Pd	1.5	0.2
Au	6.3	0.5

(b)

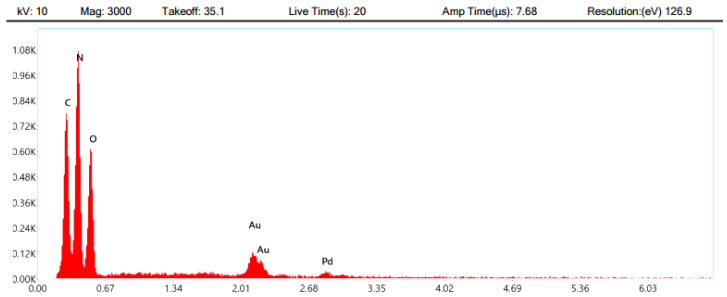

(c)

Fig. 8. (a) FESEM image showing the uniform spherical morphology of N-CQDs (Sample 1); (b) EDX elemental analysis; (c) Concentration plots

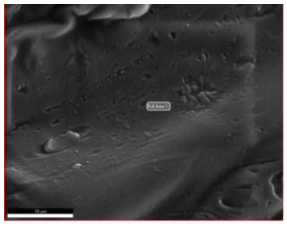

(a)

eZAF Quant Result - Analysis Uncertainty: 10.46 %

Element	Weight %	Atomic %
C	55.0	62.2
N	14.5	14.0
O	27.9	23.6
Au	2.6	0.2

(b)

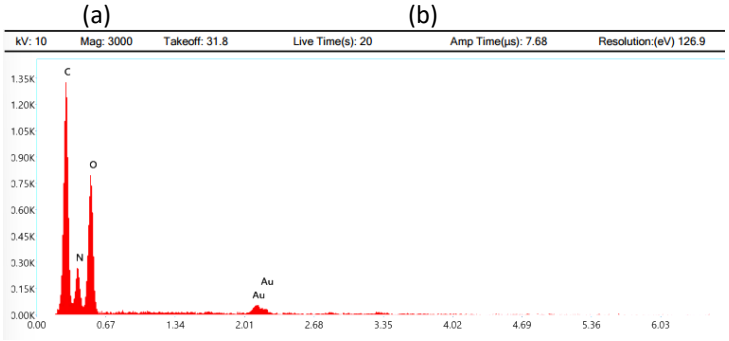

(c)

Fig. 9. FESEM image showing the uniform spherical morphology of N-CQDs (Sample 6)); (b) EDX elemental analysis; (c) Concentration plots

Energy-Dispersive X-ray (EDX) analysis confirmed the presence of carbon, nitrogen, and oxygen in the synthesized N-CQDs, validating successful nitrogen doping and oxygen functionalization. The EDX spectra for both samples displayed distinct peaks for these elements, indicating effective incorporation during the synthesis process. Nitrogen doping is particularly significant, as it alters the electronic structure of the N-CQDs, influencing their bandgap and enhancing their optical properties. Surface functionalization and elemental doping collectively contribute to the fine-tuning of these nanomaterials, making them highly adaptable for a range of advanced applications [23].

TEM images of Sample 1 (Figure 10) and Sample 6 (Figure 11), both synthesized via the hydrothermal method, revealed distinct differences in particle size distribution. TEM analysis showed that Sample 1 had a smaller average particle size of approximately 3.47 nm, with individual particles ranging from 2.34 nm to 4.33 nm. The particles displayed a relatively uniform size distribution and minimal aggregation. In contrast, Sample 6 exhibited a larger average particle size of about 4.06 nm, with particle sizes ranging from 2.78 nm to 5.09 nm, and showed more noticeable aggregation in the TEM micrographs.

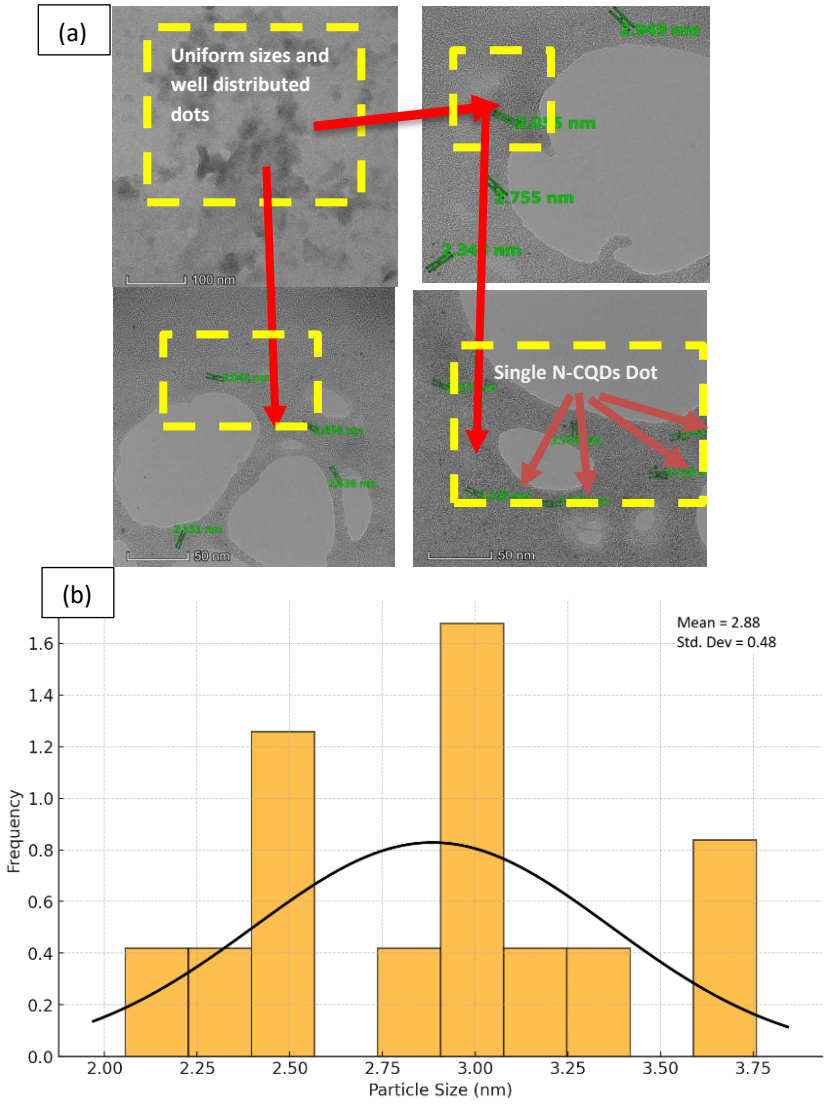

Fig. 10. (a) TEM images showing the uniform spherical morphology of N-CQDs (Sample 1); (b) Particle size distribution

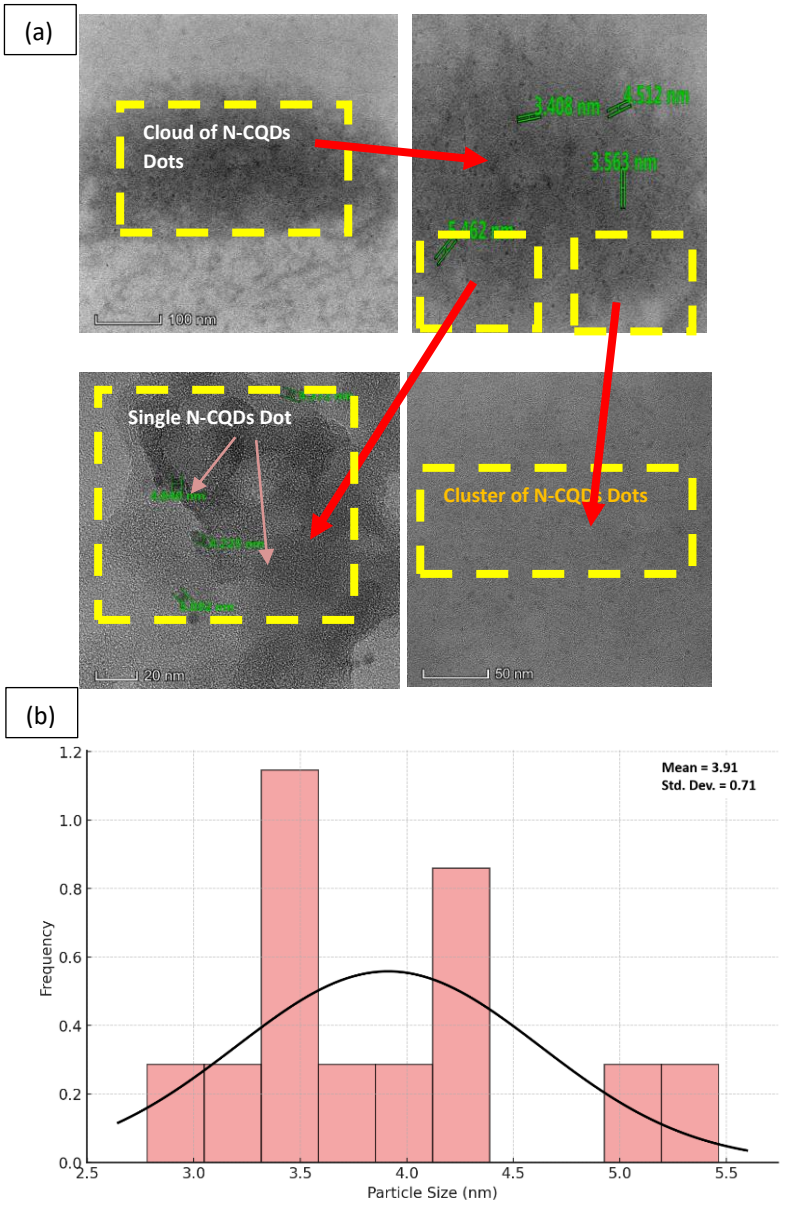

Fig. 11. (a) TEM images showing the uniform spherical morphology of N-CQDs (Sample 6); (b) Particle size distribution

Aggregation of nanoparticles can significantly influence their optical properties, often resulting in increased scattering losses and decreased fluorescence efficiency. The differences in particle size distribution were further validated by the corresponding histograms. For Sample 1, the yellow histogram showed a mean particle size of 2.88 nm with a standard deviation of 0.48 nm, indicating a more uniform and tightly distributed particle size. In comparison, Sample 6's pink histogram indicated a mean particle size of 3.91 nm with a standard deviation of 0.71 nm, reflecting a broader size distribution and larger average particle size. These results, supported by both TEM micrographs and histograms, confirm the disparity in uniformity and aggregation behavior between the two samples. The broader size distribution and increased aggregation observed in Sample 6 may contribute to heterogeneous optical behavior, potentially limiting its suitability for applications requiring consistent and uniform particle characteristics.

4. Conclusions

This study successfully synthesized nitrogen-doped carbon quantum dots (N-CQDs) via an eco-friendly hydrothermal method. The optimization of synthesis parameters using the Design of Experiment (DOE) approach led to the production of high-quality N-CQDs with excellent optical properties and colloidal stability. The N-CQDs exhibited strong photoluminescence, small particle sizes below 6 nm, and a maximum band gap of 5.813 eV, making them suitable for bioimaging, sensing, and optoelectronics. Future research should focus on improving N-CQD performance through surface functionalization and surfactant modifications to enhance stability and optical properties. Scaling up the synthesis process while maintaining quality is essential for real-world applications. Additionally, deeper studies on biocompatibility, toxicity, and interactions with biomolecules will be crucial for medical and biosensing applications. Advanced characterization techniques such as HRTEM and improved purification methods like dialysis can further refine N-CQD properties. By addressing these aspects, N-CQDs can be developed into versatile materials for applications in nanotechnology, healthcare, and sustainable technologies.

Acknowledgment

This research was funded by a grant from Universiti Teknikal Malaysia Melaka under MTUN Strategic Research Grant with Project Number: MTUN/2024/UTEM-FTKIP/CRG/MS0006.

References

[1] P. Zhao, B. Jin, Q. Zhang and R. Peng, "High-Quality Carbon Nitride Quantum Dots on Photoluminescence: Effect of Carbon Sources," Langmuir 37, no. 5 (2021): 1760-1767. https://doi.org/10.1021/acs.langmuir.0c02966

[2] H.-L. Yang, L.-F. Bai, Z.-R. Geng, H. Chen, L.-T. Xu, Y.C. Xie, D.-J. Wang, H.-W. Gu and X.-M. Wang, "Carbon Quantum Dots: Preparation, Optical Properties, and Biomedical Applications," Materials Today Advances 18, (2023): 100376. https://doi.org/10.1016/j.mtadv.2023.100376

[3] H. Fan, M. Zhang, B. Bhandari and C.-h. Yang, "Food Waste as a Carbon Source in Carbon Quantum Dots Technology and Their Applications in Food Safety Detection," Trends in Food Science & Technology 95, (2020): 86-96. https://doi.org/10.1016/j.tifs.2019.11.008

[4] S. Wahyudi, A. Bahtiar, C. Panatarani and Anas, Risdiana, "Recent Advanced Carbon Dots Derived Natural Products and Aptasensor-Based Carbon Dots for Detection of Pesticides," Sensing and Bio-Sensing Research 41, (2023): 100576. https://doi.org/10.1016/j.sbsr.2023.100576

[5] X.T. Zheng, A. Ananthanarayanan, K.Q. Luo and P. Chen, "Glowing Graphene Quantum Dots and Carbon Dots: Properties, Syntheses, and Biological Applications," Small 11, no. 14 (2014): 1620-1636. https://doi.org/10.1002/smll.201402648

[6] B. Vercelli, R. Donnini, F. Ghezzi, A. Sansonetti, U. Giovanella and B.La Ferla," Nitrogen-Doped Carbon Quantum Dots Obtained Hydrothermally from Citric Acid and Urea: The Role of the Specific Nitrogen Centers in Their Electrochemical and Optical Responses," Electrochimica Acta 387, (2021): 138557. https://doi.org/10.1016/j.electacta.2021.138557

[7] S. Šafranko, K. Janđel, M. Kovačević, A. Stanković, M.D. Sikirić, Š. Mandić, A. Széchenyi, L.G. Obrovac, M. Leventic, I. Strelec, K. Aladic and S. Jokić, "A Facile Synthetic Approach Toward Obtaining N-Doped Carbon Quantum Dots from Citric Acid and Amino Acids, And Their Application In Selective Detection of Fe (III) ions," Chemosensors 11, no. 4 (2023): 205. https://doi.org/10.3390/chemosensors11040205

[8] N. Ngafwan, H. Rasyid, E.S. Abood, W.K. Abdelbasset, S.G. Al-Shawi, D. Bokov and A.T. Jalil, "Study on Novel Fluorescent Carbon Nanomaterials in Food Analysis," Food Science and Technology 42, (2021): e37821. https://doi.org/10.1590/fst.37821

[9] A. Kumari, A. Kumar, S.K. Sahu and S. Kumar, "Synthesis of Green Fluorescent Carbon Quantum Dots Using Waste Polyolefins Residue for Cu^{2+} Ion Sensing and Live Cell Imaging," Sensors and Actuators B: Chemical 254, (2018): 197-205.
https://doi.org/10.1016/j.snb.2017.07.075

[10] S.Y. Lim, W. Shen and Z. Gao, "Carbon Quantum Dots and Their Applications," Chemical Society Reviews 44 (2015): 362-381.
https://doi.org/10.1039/c4cs00269e

[11] N. Murugan, M. Prakash, M. Jayakumar, A. Sundaramurthy and A.K. Sundramoorthy, "Green Synthesis Of Fluorescent Carbon Quantum Dots from *Eleusine Coracana* and Their Application as a Fluorescence 'Turn-Off' Sensor Probe for Selective Detection of Cu^{2+}," Applied Surface Science 476 (2019): 468-480.
https://doi.org/10.1016/j.apsusc.2019.01.090

[12] Y. Zhang, R. Yuan, M. He, G. Hu, J. Jiang, T. Xu, L. Zhou, W. Chen, W. Xiang and X. Liang, "Multicolour Nitrogen-Doped Carbon Dots: Tunable Photoluminescence and Sandwich Fluorescent Glass-Based Light-Emitting Diodes," Nanoscale 9, 45 (2017): 17849-17858.
https://doi.org/10.1039/c7nr05363k

[13] A. Tadesse, M. Hagos, D. RamaDevi, K. Basavaiah and N. Belachew, "Fluorescent-Nitrogen-Doped Carbon Quantum Dots Derived from Citrus Lemon Juice: Green Synthesis, Mercury(II) Ion Sensing, and Live Cell Imaging," ACS Omega 5, 8 (2020): 3889–3898.
https://doi.org/10.1021/acsomega.9b03175

[14] S. Sharma and P. Chowdhury, "Fluorescence Signal from Carbon Quantum Dots Synthesized from Natural Resources," Materials Today: Proceedings (2023).
https://doi.org/10.1016/j.matpr.2023.05.676

[15] M. Rana and P. Chowdhury, "L-Glutathione Capped CdSeS/ZnS Quantum Dot Sensor for the Detection of Environmentally Hazardous Metal Ions," Journal of Luminescence 206 (2019): 105-112.
https://doi.org/10.1016/j.jlumin.2018.10.060

[16] D. Sengottuvelu, A.K. Shaik, S. Mishra, H. Ahmad, M. Abbaszadeh, N.I. Hammer and S. Kundu, "Multicolor Nitrogen-Doped Carbon Quantum Dots for Environment-Dependent Emission Tuning," ACS Omega 7, 31 (2022): 27742-27754.
https://doi.org/10.1021/acsomega.2c03912

[17] Y. Su, M. Xie, X. Lu, H. Wei, H. Geng, Z. Yang and Y. Zhang, "Facile Synthesis and Photoelectric Properties of Carbon Dots with Upconversion Fluorescence Using Arc-Synthesized Carbon By-Products," RSC Advances 4, 10 (2014): 4839-4842.
https://doi.org/10.1039/c3ra45453c

[18] X. Liu, H.-B. Li, L. Shi, X. Meng, Y. Wang, X. Chen, H. Xu, W. Zhang, X. Fang and T. Ding, "Structure and Photoluminescence Evolution of Nanodots During Pyrolysis of Citric Acid: From Molecular Nanoclusters to Carbogenic Nanoparticles," Journal of Materials Chemistry C 5, 39 (2017): 10302-10312.
https://doi.org/10.1039/c7tc03429f

[19] F. Wang, P. Chen, Y. Feng, Z. Xie, Y. Liu, Y. su, Q. Zhang, Y. Wang, K. Yao, W. Lv and G. Liu, "Facile Synthesis of N-Doped Carbon Dots/g-C_3N_4 Photocatalyst with Enhanced Visible-Light Photocatalytic Activity for the Degradation of Indomethacin," Applied Catalysis B: Environmental 207 (2017): 103–113.
https://doi.org/10.1016/j.apcatb.2017.02.024

[20] Y. Yang, W. Kong, H. Li, J. Liu, M. Yang, H. Huang, Y. Liu, Z. Wang, Z. Wang, T.-K. Sham, J. Zhong, C. Wang, Z. Liu, S.-T. Lee and Z. Kang, "Fluorescent N-Doped Carbon Dots as In Vitro and In Vivo Nanothermometer," ACS Applied Materials & Interfaces 7, 49 (2015): 27324-27330.
https://doi.org/10.1021/acsami.5b08782

[21] G. Ramalingam, P. Kathirgamanathan, G. Ravi, T. Elangovan, B. Arjun, N. Manivannan and K. Kasinathan, "Quantum Confinement Effect of 2D Nanomaterials," In Quantum Dots-Fundamental and Applications. IntechOpen, 2020.
https://doi.org/10.5772/intechopen.90140

[22] J. Kong, Y. Wei, F. Zhou, L. Shi, S. Zhao, M. Wan and X. Zhang, "Carbon Quantum Dots: Properties, Preparation, and Applications," Molecules 29, 9 (2024): 2002.
https://doi.org/10.3390/molecules29092002

[23] M.H. Abo Zaid, N. El-Enany, A.E. Mostafa, G.M. Hadad and F. Belal, "Use of Green Fluorescent Nano-Sensors for the Determination of Furosemide in Biological Samples and Pharmaceutical Preparations," BMC Chemistry 17, 1 (2023): 25.
https://doi.org/10.1186/s13065-023-00937-y